

On the Unsteady Free Convective Flow with Radiative Heat Transfer of Sisko Fluid

Akindele Michael Okedoye

Department of Mathematics and Computer Science, Federal University of Petroleum Resources
PMB 1221, Effurun, Nigeria. E-mail: okedoye.akindele@fupre.edu.ng

Abstract

An approximate numerical solution of an unsteady free convective flow with radiative heat transfer past a flat plate moving through a binary mixture for a Sisko fluid has been obtained by solving the governing equations using numerical technique. Numerical calculations are carried out for different values of dimensionless parameters and an analysis of the results obtained shows that the flow is influenced appreciably by the chemical reaction, heat source, suction/injection at the wall and also the influence of Dufour and Soret in Sisko fluid.

Keywords: *Boundary layer flow; Radiative heat; Binary mixture; Arrhenius kinetics; Porous plate; Dufour and Soret; Sisko fluid*

1. Introduction

It is now well known that most of the fluids in industry do not hold commonly accepted assumption of a linear relationship between the stress and the rate of strain and, thus are characterized as non-Newtonian fluids. Rheological fluids have wide coverage in medicine, engineering, and industry. For example, they are important in polymeric and food processes. The Couette flow configuration for rotating frame and porous space has a growing interest among recent modelers and computer scientists. This is in fact because of the occurrence of such flows in petroleum, magnetohydrodynamic (MHD) generators, geothermal processes, underground energy, and metallurgical processes. It is a well-established argument that stretching, bearing, and fluid-driven shear play a key role in synovial joints. The inadequacies of the classical Navier–Stokes theory to describe rheological complex fluids such as polymer solution, blood, paints, certain oils and greases, have led to the development of several theories of non-Newtonian fluids. In this theory, relation connecting shear stress and shear rate is not usually linear; that is, the ‘viscosity’ of a non-Newtonian fluid is not constant at a given temperature and pressure, but depends on the rate of shear or on the previous kinematic history of the fluid [1]. Hence, there is no constitutive relation able to predict all non-Newtonian behaviors that can occur.

Nalim et al.[2] examined the oscillatory Couette flow mechanical shear loader to simulate in vitro fluid-driven

shear. This flow configuration generates shear since the loader enhances understanding of mechanotransduction in the joint tissue. Prasad and Kumar [3] implemented a boundary layer assumption for the analysis of MHD oscillatory Couette flow with a porous space. The hydromagnetic Couette flow of viscous fluid in a rotating channel was investigated by Beg et al.[4–5]. The lower plate of the channel exhibited non-torsional oscillation. Seth et al.[6–7] and Guria et al.[8] addressed MHD Couette flows in a porous channel and rotating frame.

It is now known that non-Newtonian fluids are more suited in industrial and physiological applications than Newtonian fluids. The expressions for these fluids in a rotating frame are very complicated. Hence, numerical and analytical techniques are implemented to describe the flow of rheological materials by means of various aspects [9–16]. The purpose of the current work is to advance the knowledge in this area. Thus, a nonlinear problem for the MHD Couette flow of a Sisko fluid between two infinite non-conducting parallel plates in a rotating frame is formulated.

The understanding of physics involved in the flows of non-newtonian fluids can have immediate effects on polymer processing, coating, ink-jet printing, micro fluidics, geological flows in the earth mantle, homodynamic, the flow of colloidal suspensions, liquid crystals, additive suspensions, animal blood, turbulent shear flows and many others. In view of this, a lot of interest has been shown towards the study of non-Newtonian flows and hence extensive literature regarding analytic and numerical solutions is available on the topic. It is also accepted now that in general, the governing equations of non-Newtonian fluids are highly non-linear and of higher order than the Navier–Stokes equations. Because of the non-linearity and the inapplicability of the superposition principle, the exact solutions are even difficult to be obtained for the case of viscous fluids [17–19].

Several excellent studies of stretching flows in materials processing were presented by Karwe and Jaluria [22]. Ahmed [23] examined the Similarity solution in MHD: Effects of thermal diffusion and diffusion thermo non free convective heat and mass transfer over a stretching surface

considering suction or injection. Tsai and Huang investigated [24] the Numerical study of Soret and Dufour

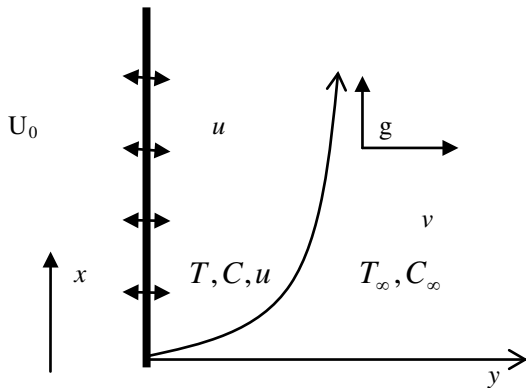


Fig. 1: Flow configuration and coordinate system.

effects on heat and mass transfer from natural convection flow over a vertical porous medium with variable wall heat fluxes.

Therefore, the objective of this work is not only to investigate the Dufour and Soret effects on an unsteady free convection flow with radiative heat transfer past a flat plate but also to study radiation and chemical reaction effect of a Sisko fluid which was not taken into consideration by the previous researchers.

2. Basic Equations

The basic equations governing the motion of an incompressible fluid neglecting the thermal effects are

$$\text{div}V = 0, \tag{1}$$

$$\rho \frac{DV}{Dt} = \rho f - \nabla p + \text{div}S \tag{2}$$

where V is the velocity vector ρ is the constant density, f is the body force per unit mass, p is the dynamic pressure, S is the extra stress tensor and $\frac{DV}{Dt}$ is the material time derivative. The constitutive equation for incompressible Sisko fluid Sisko (1958), Siddiqui et al. (2009), Mekheimer and El Kot (2012) is given by

$$S = \left[a + b \left(\sqrt{\frac{1}{2} \text{tr}A_1^2} \right)^{n-1} \right] A_1 \tag{3}$$

Where A_1 is the Rivlin-Ericksen tensor:

$$A_1 = L + L^T, \quad L = \text{grad}V \tag{4}$$

a, b are material constants and n is the fluid behaviour index. If $a = 0$, equation for the power law fluid model

is obtained and, if $b = 0$, equation for Newtonian fluid is obtained.

Using (3) and (4)

$$S(y, t) = \left(a + b \left| \frac{\partial u}{\partial y} \right|^{n-1} \right) \frac{\partial u}{\partial y} \tag{5}$$

3. Problem Formulation

Consider an unsteady one – dimensional convective flow of a viscous incompressible fluid with radiative heat transfer and chemical reaction past a flat plate moving through a binary mixture (Fig. 1).

Let the x -axis be taken along the plate in the vertically upward direction and the y -axis be taken normal to it. For the problem considered here we define the velocity and the stress fields of the following form

$$V = [u(y, t), 0, 0], \quad S = S(y, t) \tag{6}$$

According to (Tan and Masuoka 2005a 2005b), the constitutive relationship between the pressure drop and the velocity for the unidirectional flow of a Sisko fluid is

$$\frac{\partial p}{\partial x} = -\frac{\gamma}{k} \left(v + h \left| \frac{\partial u}{\partial y} \right|^{n-1} \right) u \tag{7}$$

Where $k (> 0)$ and $\gamma (0 < \gamma < 1)$ are the permeability and porosity.

The pressure gradient in equation (7) is regarded as a measure of the flow resistance in the bulk of the porous medium. If R_x is a measure of the flow resistance offered by the solid matrix in the x -direction then R_x through equation (7) is inferred by

$$R_x = -\frac{\gamma}{k} \left(v + h \left| \frac{\partial u}{\partial y} \right|^{n-1} \right) u \tag{8}$$

We take the body force

$$\rho f = g\beta(T - T_\infty) + g\beta(C - C_\infty) + R_x \tag{9}$$

The physical variables are functions of y and t only. Therefore, the only velocity component is in y - direction. By above assumption, under (6), the continuity equation (1) could be written as

$$\frac{\partial v}{\partial y} = 0,$$

from relations (2) - (9) we have the momentum equation

$$\rho \left(\frac{\partial u}{\partial t} + v \frac{\partial u}{\partial y} \right) = \frac{\partial}{\partial y} \left[\left(v + h \left| \frac{\partial u}{\partial y} \right|^{n-1} \right) \frac{\partial u}{\partial y} \right] + g\beta(T - T_\infty) + g\beta(C - C_\infty) - \frac{\gamma}{k} \left(v + h \left| \frac{\partial u}{\partial y} \right|^{n-1} \right) u \quad (10)$$

Under the Boussinesq's approximation, the fluid energy and species equations in the neighbourhood of the plate is described by the following respectively

$$\rho c_p \left(\frac{\partial T}{\partial t} + v \frac{\partial T}{\partial y} \right) = k \frac{\partial^2 T}{\partial y^2} + Q - 4\sigma\alpha T^4 + \frac{Dk_T}{c_s} \frac{\partial^2 C}{\partial y^2} \quad (11)$$

$$\frac{\partial C}{\partial t} + v \frac{\partial C}{\partial y} = D_m \frac{\partial^2 C}{\partial y^2} - R_A + \frac{Dk_T}{T_m} \frac{\partial^2 T}{\partial y^2} \quad (12)$$

Where $Q = (-\Delta H)R_A$ is the heat of chemical reaction; ΔH is the activation enthalpy. $R_A = k_r C_A^n$ for nth order irreversible reaction. We employed chemical reaction of Arrhenius type of the n^{th} order irreversible reaction given by,

$$R_A = a_1 e^{-E/R_G T} (C - C_\infty)^r \quad (13)$$

Where a_1 is the pre exponential factor defined by frequency of collision ω and orientation factor p as $a_1 = \omega p$, R_G is the universal gas constant.

The appropriate initial and boundary conditions relevant to the problem are

$$\begin{aligned} t \leq 0, u = v = 0, T = T_w, C = C_w \quad \forall y \\ t > 0 \begin{cases} u(0, t) = U(t), T(0, t) = T(t) \\ C(0, t) = C(t), v = v(t) \\ u \rightarrow 0, T \rightarrow T_\infty, C \rightarrow C_\infty \text{ as } y \rightarrow \infty \end{cases} \quad (14) \end{aligned}$$

where U_0 is the plate characteristic velocity.

It is interesting to observe that for $a = 0$ ($b \neq 0, n \neq 1$), the above equation will be equation of power-law fluids and for $b = 0$ ($a \neq 0, n = 1$) it will be equation of Newtonian fluid.

We introduce a similarity variables parameter σ , which is a time dependent length scale, as

$$\sigma = \sigma(t)$$

In term of this length scale, appropriate solution of the eqn(1) is considered to be in the following form

$$v(y, t) = v(t) = -v_0 \frac{v}{\sigma(t)} \quad (15)$$

$v_0 (> 0)$ is the suction velocity.

We now define conveniently the following dimensionless quantities;

$$\left. \begin{aligned} \eta &= \frac{y}{\sigma(t)} \\ u &= U_0 \sigma^{2m+2} f(\eta) \\ \frac{T - T_\infty}{\epsilon T_\infty} &= \sigma^{2m} \theta(\eta) \\ \frac{C - C_\infty}{C_w - C_\infty} &= \sigma^{2m} \phi(\eta) \end{aligned} \right\} \quad (16)$$

Where m is a non-negative integer. Here $\sigma_* = \frac{\sigma(t)}{\sigma_0}$, σ_0 is the value of σ at $t = 0$.

Now, using these quantities, we have

$$\begin{aligned} R_A &= b_1 \phi(\eta)^r e^{1+\epsilon\theta(\eta)} \\ Q &= \frac{\alpha U_0}{d} b_1 \phi(\eta)^r e^{1+\epsilon\theta(\eta)} \\ b_1 &= \frac{a_1 (C_w - C_\infty)^r \sigma^{2mr} e^{\frac{1}{\epsilon}}}{\sigma_0^{2mr}} \end{aligned}$$

Substituting for R_A and Q , and using (15) and (16), the equations (10) – (12) together with the boundary conditions becomes

$$\frac{\sigma(t)}{v} \frac{d}{dt} \sigma(t) (2m\phi(\eta) - \eta\phi'(\eta)) - v_0\phi'(\eta) = \frac{1}{Sc} \phi''(\eta) - \beta\phi(\eta)^r e^{1+\epsilon\theta(\eta)} + Sr\theta''(\eta) \quad (17)$$

$$\begin{aligned} \frac{\sigma(t)}{v} \frac{d}{dt} \sigma(t) (2m\theta(\eta) - \eta\theta'(\eta)) - v_0\theta'(\eta) \\ = \frac{1}{Pr} \theta''(\eta) - \lambda\phi(\eta)^r e^{1+\epsilon\theta(\eta)} + Du\theta''(\eta) \quad (18) \end{aligned}$$

$$\begin{aligned} \frac{\sigma(t)}{v} \frac{d}{dt} \sigma(t) ((2m+2)f(\eta) - \eta f'(\eta)) - v_0 f'(\eta) = (1 + n\delta f'(\eta)^{n-1}) f''(\eta) \\ + Grt\theta(\eta) + Grc\phi(\eta) \quad (19) \end{aligned}$$

$$-c(1 + \delta f'(\eta)^{n-1}) f'(\eta)$$

Where

$$\begin{aligned} Grt &= \frac{g\beta_\tau \epsilon T_\infty \sigma_0^2}{\mu U_0}, Grc = \frac{g\beta_c (C_w - C_\infty) \sigma_0^2}{\mu U_0}, \delta = \frac{b}{a} \left(\frac{U_0}{\sigma_0} \left(\frac{\sigma(t)}{\sigma_0} \right)^{2m+1} \right)^{n-1} \\ Sr &= \frac{D_{kT} \epsilon T_\infty}{v (C_w - C_\infty) T_m}, Du = \frac{D_{kT} (C_w - C_\infty)}{\epsilon k T_\infty c_s}, \beta = \frac{b_1}{v} \sigma_0^{2m} \sigma(t)^{2-2m}, \lambda = \gamma \beta \end{aligned}$$

$$\gamma = \frac{\alpha U_0}{\rho c_p \epsilon T_\infty d}, Sc = \frac{\nu}{Dm}, Pr = \frac{k}{\mu c_p}$$

Now, equations (16) – (19) are locally similar except the term $\frac{\sigma(t)}{\nu} \frac{d}{dt} \sigma(t)$, where t appears explicitly. Thus the local similarity condition requires that

$$\frac{\sigma(t)}{\nu} \frac{d}{dt} \sigma(t) = S \text{ (constant)} \tag{20}$$

Integrating (20), we have

$$\sigma(t) = \sqrt{2S\nu t} + I$$

At $t = 0, \sigma(0) = 0 \Rightarrow I = 0$. Thus

$$\sigma(t) = \sqrt{2S\nu t} \tag{21}$$

From (21), we choose $S = 2$ without loss of generality.

Therefore the length scale $\sigma(t)$ is given as

$$\sigma(t) = 2\sqrt{\nu t}$$

Letting $\eta = \eta' - \frac{\nu_0}{2}$, after dropping prime ($'$) equation (17) – (19) becomes

$$\phi''(\eta) + 2Sc\eta\phi'(\eta) - 4mSc\phi(\eta) - \beta Sc\theta(\eta)^r e^{\frac{\theta(\eta)}{1+\epsilon\theta(\eta)}} + ScSr\theta''(\eta) = 0 \tag{22}$$

$$\theta''(\eta) + 2Pr\eta\theta'(\eta) - 4mPr\theta(\eta) - \lambda Pr\theta(\eta)^r e^{\frac{\theta(\eta)}{1+\epsilon\theta(\eta)}} + PrDu\theta''(\eta) = 0 \tag{23}$$

$$(1 + n\delta f'(\eta)^{n-1})f''(\eta) + 2\eta f'(\eta) - (4m + 4)f(\eta) + Grt\theta(\eta) + Grc\phi(\eta) - c(1 + \delta f'(\eta)^{n-1})f(\eta) = 0 \tag{24}$$

Correspondingly, the boundary conditions becomes

$$\begin{aligned} f(0)=1, \theta(0)=1, \phi(0)=1 \\ f(\eta) \rightarrow 0, \theta(\eta) \rightarrow 0, \phi(\eta) \rightarrow 0 \text{ as } \eta \rightarrow \infty \end{aligned} \tag{25}$$

The equations (22) – (25) are similar and was solved numerically for various values of the parameters entering in to the problem. From the process of numerical computation, other physical quantities of interest in this work namely, the skin friction parameter (τ) and the Nusselt number (Nu) and Sherwood number (Sh) which are proportional to $\tau = -f'(0)$, $Nu = \theta'(0)$ and $Sh = \phi'(0)$, are also sorted out and their numerical values are presented in tabular form.

3. Numerical procedure

Numerical solution to the transformed set of non-linear ordinary differential equations (22)–(24) with boundary conditions in (25) were obtained, using a seventh-eighth order continuous Runge-Kutta method along with boundary value problem sub method ‘trapezoid methods (traprich)’ that use Richardson extrapolation enhancement [30 - 35]. Because of end-point singularities, midpoint (middefer) methods with deferred correction enhancement are coupled together to handle harmless end-point singularities, with B, d, $G_c, G_r, \gamma, Ra, Da, \theta_w, \phi_w, c, b, n, Sc$, and Pr as prescribed parameters. The computation was carried out using MAPLE 18. Grid-independence studies show that the computational domain $0 < \eta < \eta_\infty$ can be divided into intervals each of uniform step size which equals 0.02. This reduces the number of points between $0 < \eta < \eta_\infty$ without sacrificing accuracy. The value $\eta_\infty = 10$ was found to be adequate for all the ranges of parameters studied here.

Skin-Friction: We now study skin-friction from velocity field. It is given by

$$c_f = \frac{T_f}{\rho u_\omega v_\omega} = \frac{d^2}{dy^2} u(y, t) \Big|_{y=0}, \tau_f = \mu \frac{du}{dy} \Big|_{y=0}$$

Therefore

$$\tau = - \frac{df(\eta)}{d\eta} \Big|_{\eta=0} \tag{26}$$

Nusselt Number: In non-dimensional form, the rate of heat transfer at the wall is computed from Fourier's law and is given by

$$\begin{aligned} Nu = \frac{q_\omega v}{(T_\omega - T_\infty)Kv_\omega} = \frac{-d}{dy} \theta(y, t) \Big|_{y=0}, \\ q_\omega = -K \frac{dT}{dy} \Big|_{y=0}, \end{aligned}$$

Therefore,

$$Nu = \frac{d\theta(\eta)}{d\eta} \Big|_{\eta=0} \tag{27}$$

Sherwood Number: The rate of mass transfer at the wall which is the ratio of length scale to the diffusive boundary layer thickness is given by

$$Sh = \frac{J_\omega v}{(c_\omega - c_\infty) D v_\omega} = - \left. \frac{d\phi}{dy} \right|_{y=0},$$

$$J_\omega = - D \left. \frac{d\phi}{dy} \right|_{y=0}$$

Which implies

$$Sh = \left. \frac{d\phi(\eta)}{d\eta} \right|_{\eta=0} \quad (28)$$

4. Results and discussion

For the purpose discussing the effect of various parameters on the flow behavior near the plate, numerical calculation have been carried out for different values of $Grt, Grc, \delta, \beta, \lambda, v_0, Sr, Du$ and c and for fixed values of Sc, Pr and r . In order to point out the effects of various parameters on flow characteristic, to be realistic, the values of Schmidt number (Sc) are chosen for hydrogen ($Sc = 0.22$), at temperature $25^\circ C$ and one atmospheric pressure. The values of Prandtl number is chosen to be $Pr = 0.71$ which represents air at temperature $25^\circ C$ and one atmospheric pressure. Expression for β indicate that $r = 1$. Attention is focused on positive values of the buoyancy parameters i.e. Grashof number $Grt > 0$ (which corresponds to the cooling problem) and solutal Grashof number $Grc > 0$ (which indicates that the chemical species concentration in the free stream region is less than the concentration at the boundary surface). The cooling problem is often encountered in engineering applications; for example in the cooling of electronic components and nuclear reactors. It is should be mentioned here that $Da > 0$ indicates an increase in the chemical reaction rate (note: $\beta = Da$). All parameters are primarily chosen as follows: $m = 1, n = 1, r = 1, Sc = 0.22, Pr = 0.71, Grt = 5.0, Grc = 5.0, \delta = 0.8, \beta = -2.0, \lambda = 0.1, v_0 = 0.3, Sr = 3, Du = 1$,

unless otherwise stated. The effect of each flow parameters on the concentration, temperature and velocity distribution of the flow field are presented with the help of concentration profile (Figures (2) – (5)), temperature profile (Figures (6) – (10)) and velocity profiles (Figures (11) - (16)).

4.1. Concentration distribution. The concentration distribution of the flow field in presence of foreign species, such as hydrogen ($Sc = 0.22$) is shown in Figures (2) – (5). It is affected by four flow parameters, namely Damköhler number (β), suction parameter (v_0), Soret number (Sr) and heat generation (λ).

4.2. Temperature field. The temperature of the flow field is mainly affected by four five parameters, namely, Damköhler number (Da), suction parameter (c), radiation parameter (Ra) and Dufour number (Du). The effects of these parameters on the temperature field are shown graphically in figures ((6) – (9)).

4.3. Velocity field. The velocity of the flow field is found to change more or less with the variation of the flow parameters. The effect of the flow parameters on the velocity field is analyzed with the help of Figures (10) - (13). Our attention is on the case of cooling of plate.

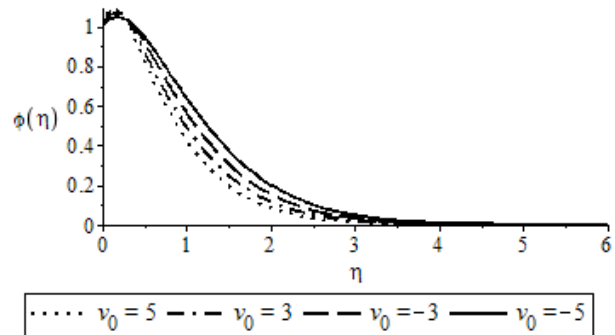


Figure 2: Concentration Profiles for various suction parameter

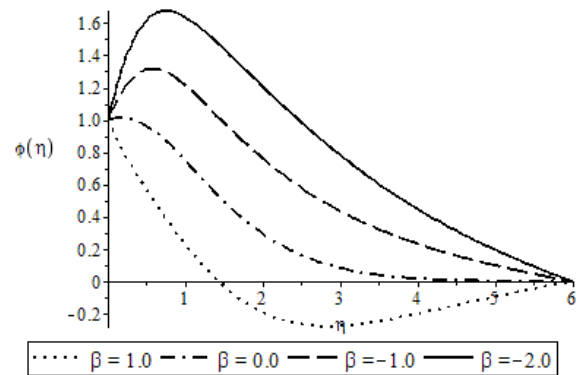


Figure 3: Concentration Profiles for various β

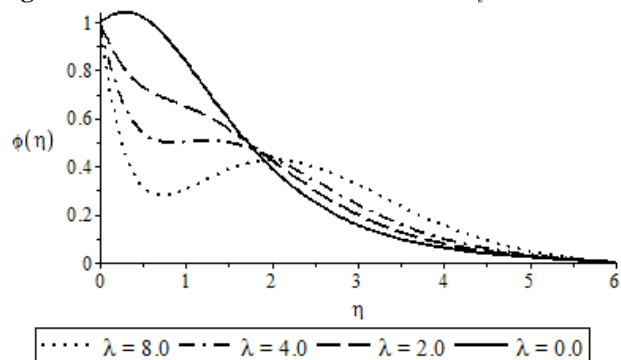


Figure 4: Concentration Profiles for combined heat absorption parameter

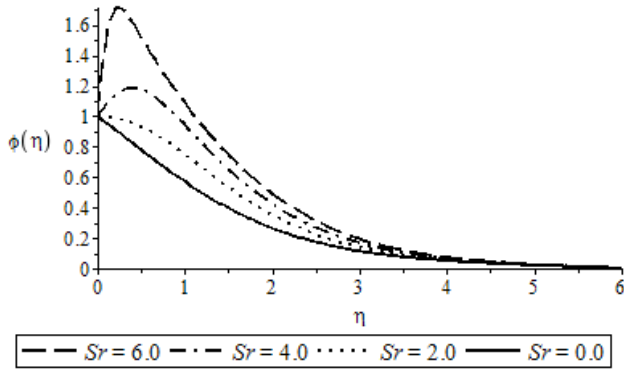


Figure 5: Concentration Profiles for various Soret number

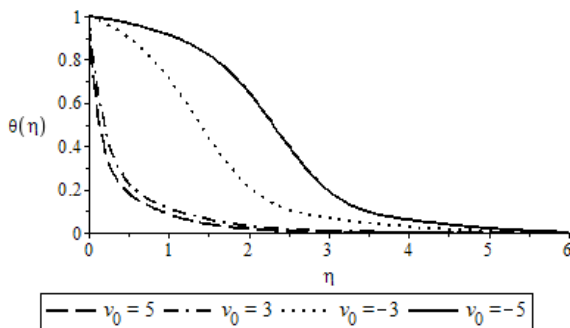


Figure 6: Temperature Profiles for various Suction parameter

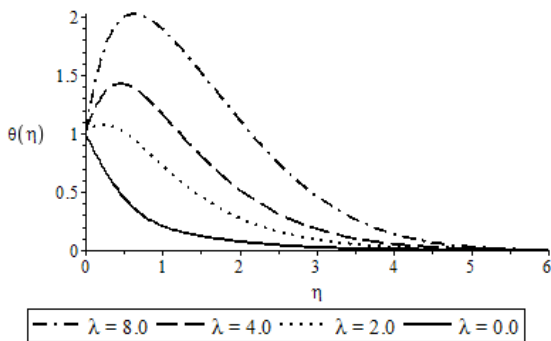


Figure 7: Temperature Profiles for combined heat reaction parameter

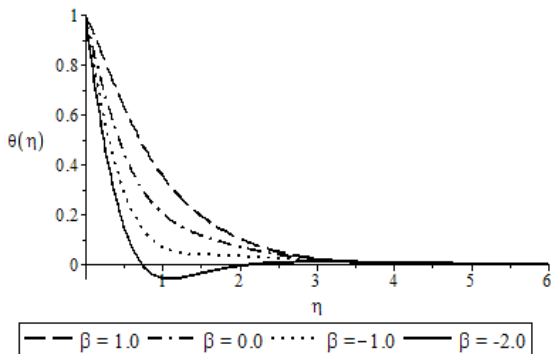


Figure 8: Temperature Profiles for various β

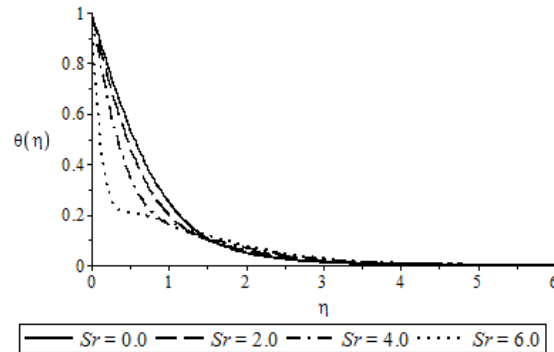


Figure 9: Temperature Profiles for various Soret number

4.1.1. Effect of suction parameter (v_0): Figure (2) shows that concentration distribution of the flow field decreases as suction increases ($v_0 > 0$), whereas the distribution of the chemical species increases with increase in injection. This phenomenon is significant within the neighborhood of the boundary. As the fluid moves away from the plate, the chemical species decay away. Specifically, suction is characterized by removal of fluid from the flow path which implies reduction in the chemical composition of the fluid. So also, for the case of injection ($v_0 < 0$) of the foreign species in to the system, the concentration of the chemical species increases as depicted by the species profile. Hence, concentration increases with an increase in injection and decrease as suction parameter increases. The same phenomenon is observed with energy distribution. But in this case, we notice that suction greatly affect thermal distribution. As suction increases temperature distribution falls considerably as shown in figure 6. The influence of suction/injection parameter is seen to affect velocity greatly. This could be infer from figure 11, that suction reduces velocity whereas injection inbring about increase in velocity with maximum velocity within the body of fluid only possible for injection ($v_0 < 0$)

4.1.2. Effect of Damköhler number (β): If the reaction occurs fastest ($Da \gg 1$) then all chemical reaching $x = L$ is degraded and hence $c(L) = 0$. If the reaction is slow compared with diffusion then the chemical can build up along the boundary ($c(L) = c_0$). In figure 3, it is observed that concentration distribution is vastly affected by the Damköhler number in the flow field. A comparative study of the curves of figure 3 shows that the concentration distribution of the flow field decreases as β becomes larger as Damköhler number increases. Thus greater Damköhler number leads to a faster decrease in concentration of the flow field. For $\beta > 0$, at $\eta \geq 1.9$ we notice a destructive chemical reaction. For lower values of

Damköhler number, the peak in the profile indicates a process of generative chemical reaction very close to the boundary and this occur for $\eta < 1$ after which the chemical species decreases away from the boundary. Increase in Damköhler number is observed to bring about increase in temperature distribution as depicted in figure 8. Temperature is significantly affected when $0 \leq \eta \leq 3.0$ after which it approaches zero. From figure 13, it could be seen that increase in Damköhler number reduces the velocity with a revers velocity possible in higher value of Damköhler number.

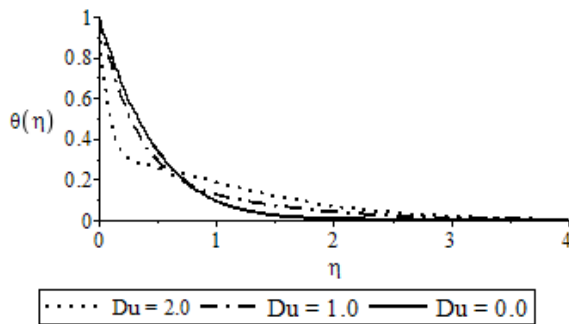


Figure 10: Temperature Profiles for various Dufour number

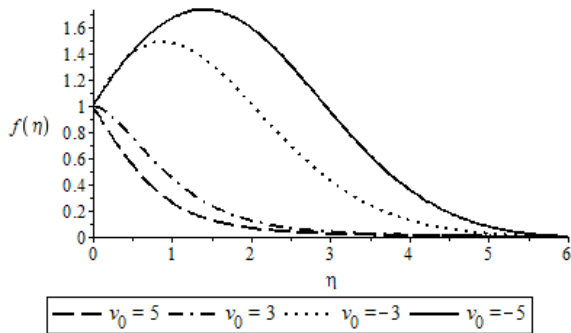


Figure 11: Variation of velocity for various suction parameters.

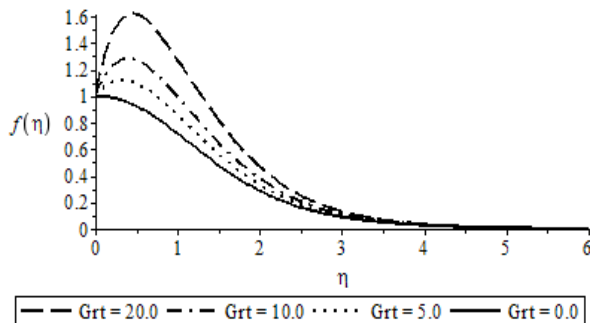


Figure 12: Variation of velocity for various values of Grt

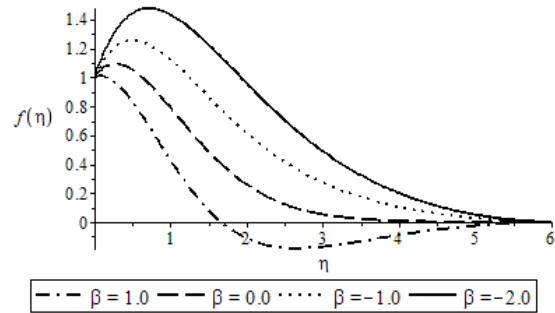


Figure 13: Variation of velocity for various values of β

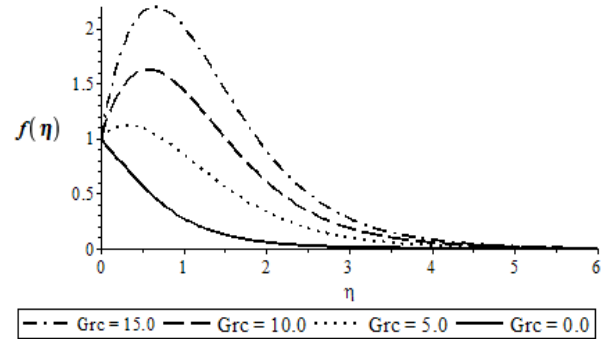


Figure 14: Variation of velocity for various values of Grc

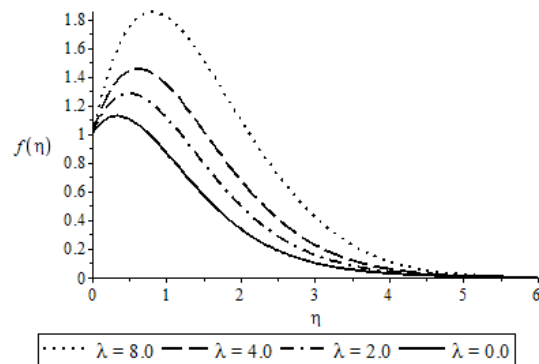


Figure 15: Velocity Profiles for combined heat reaction parameter.

4.1.3. Effect of Heat parameter (λ): The combined effect of reactivity factor (Damköhler number) and heat absorption is displayed in figure 4. The effect of heat absorption on concentration is displayed in figure 4. Two sectional flows occur with partition $0 \leq \eta \leq 1.9$ and $\eta > 1.9$. The first section shows that heat absorption reduces the concentration of the chemical species whereas in the second segment of the flow, increase in heat absorption results into an increase in concentration. In the case of thermal distribution, there exists only one regime as seen from figure 7. As heat absorption increases, the temperature of the fluid also increases. The presence of a peak in the profile indicates that maximum temperature occurs in the body of the fluid and not on the surface. This

maximum occur between $0 < \eta \leq 0.72$. The influence of heat parameter on velocity is shown in figure 15. We observed that heat absorption increases velocity as more molecules are agitated which in turn increase their mobility and hence increase in heat absorption parameter increases the velocity. Furthermore, maximum velocity with heat absorption occur below the surface.

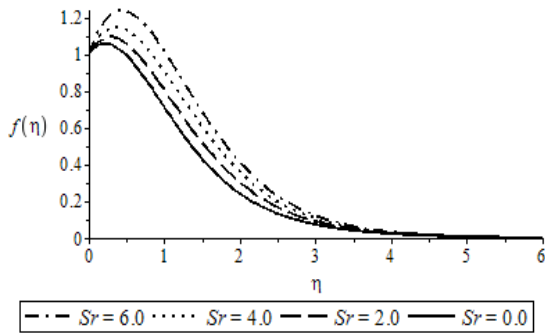


Figure 16: Velocity Profiles for various Soret number.

Table 1: Effect of Thermal and Mass buoyancy on Nusselt number

Grt	Grc	$-f'(0)$
0.0	5.0	1.145662
5.0	5.0	0.796831
10.0	5.0	0.428838
20.0	5.0	0.067438
5.0	0.0	1.350659
5.0	5.0	0.673104
5.0	10.0	-0.004449
5.0	15.0	-0.682004

4.1.4. Effect of Soret number (Sr): The thermophoresis factor has been calculated from molecular interaction potentials derived from known molecular models. The ratio of diffusion coefficient is small compared to thermo diffusion coefficient, and hence the values of Sr in our discussion is greater than one. Thus increase in thermo diffusion brings about increase in concentration. As in the case for thermal distribution, increase in Soret number decreases temperature constitution of the flow. It could be confirm from figure 9 that effect of Soret number on temperature is significant when $0 \leq \eta \leq 1.5$ and slightly significant when $1.5 < \eta \leq 3.5$ outside which the temperature becomes insignificant. Soret number, increases the velocity with maximum velocity in the body of the fluid close to the surface as shown in figure 15. The maximum for each of Soret number tilt to the right of η as Soret number increases.

4.1.5. Effect of Dufour number (Du): The influence of Dufour number on the temperature field is shown in figure (10). It could be seen that temperature reduces as the Dufour number increases when $0 \leq \eta < 0.75$. Also the thermal bopoundary layer reduces with an increase in Dufour number.

4.3.3. Effect of Grashof number for heat transfer (Grt): The effect of thermal Grashof number on the velocity of the flow field is presented in Figure (12). In the figure, we show that the Grashof number for heat transfer (Grt) accelerate the velocity of the flow field. Comparing the curves of Figure (12), it is further observed that the increase in velocity of the flow field is more significant in presence higher thermal buoyancy. Thus, heat transfer has a dominant effect on the flow field.

4.3.4. Effect of mass Grashof number (Grc): The effects of Grashof numbers for mass transfer (Grc) on the velocity of the flow field is presented in Figure (14). A study of the curves of the figure (14) shows that the Grashof number for mass transfer also accelerates the velocity of the flow field. Comparing the curves of Figure (14), it is further observed that the maximum velocity with higher mass Grashof number in cooling of surface occur in the body of the fluid.

4.4. Skin – friction, Rate of mass transfer and Heat flux. The non-dimensional skin friction (c_f), rate of mass transfer in terms of Sherwood number (Sh) and the heat flux in terms of Nusselt number (Nu), are entered in table (3) for different values of Damköhler number (Da), suction parameter (c), Shroudal number (Sr) and Schmidt number (Sc), radiation parameter (Ra) and Dufour number (Du), heat and mass Grashof numbers (Grt and Gc), H , n , and m . The effect of this parameters on the non-dimensional skin friction (c_f), rate of mass transfer in terms of Sherwood number (Sh) and the heat flux in terms of Nusselt number (Nu) as shown in table 3 is self-evident.

Table 2: Numerical values of skin friction, Nusselt and Sherwood numbers

λ	Sr	Du	r	v_0	β	$-f'(0)$	$-θ'(0)$	$-φ'(0)$
0	3.0	1.0	1	0.3	-2.0	0.67310	-0.64255	2.58124
0.2	3.0	1.0	1	0.3	-2.0	0.67843	-0.69480	2.67419
0.4	3.0	1.0	1	0.3	-2.0	0.70387	-0.94891	3.12495
0.8	3.0	1.0	1	0.3	-2.0	0.77033	-1.64986	4.35823
0.1	0.0	1.0	1	0.3	-2.0	0.78824	0.69371	1.87564
0.1	2.0	1.0	1	0.3	-2.0	0.75275	0.36092	2.04035
0.1	4.0	1.0	1	0.3	-2.0	0.71463	-0.06356	2.26170
0.1	6.0	1.0	1	0.3	-2.0	0.67310	-0.64255	2.58124
0.1	3.0	0.0	1	0.3	-2.0	0.66779	-0.24980	1.95886
0.1	3.0	0.5	1	0.3	-2.0	0.66955	-0.39497	2.18921
0.1	3.0	1.0	1	0.3	-2.0	0.67310	-0.64255	2.58124
0.1	3.0	1.5	1	0.3	-2.0	0.69831	-4.32268	8.26284
0.1	3.0	1.0	0	0.3	-2.0	0.59004	-0.80682	2.58612
0.1	3.0	1.0	1	0.3	-2.0	0.67310	-0.64255	2.58124
0.1	3.0	1.0	2	0.3	-2.0	0.69905	-0.56567	2.57002
0.1	3.0	1.0	3	0.3	-2.0	0.71003	-0.52291	2.56085
0.1	3.0	1.0	1	-0.5	-2.0	0.15003	-0.05213	0.74669
0.1	3.0	1.0	1	-0.3	-2.0	0.28964	-0.09196	1.11468
0.1	3.0	1.0	1	0.3	-2.0	0.93874	-1.23075	3.82967
0.1	3.0	1.0	1	0.5	-2.0	1.11315	-1.63319	4.66223
0.1	3.0	1.0	1	0.3	-0.2	0.67310	-0.64255	2.58124
0.1	3.0	1.0	1	0.3	-0.1	0.71102	-0.26763	2.39061
0.1	3.0	1.0	1	0.3	0.0	0.74208	0.07229	2.21284
0.1	3.0	1.0	1	0.3	0.1	0.77958	0.53171	1.96569

Nomenclature

α thermal conductivity
 u, v velocity components along x- and y- axes,
 C concentration of the fluid
 Dm diffusion coefficient
 T fluid temperature
 U_0 free steam velocity
 C_∞ free stream concentration
 T_∞ free stream temperature
 H is the non-Newtonian parameter
 Q heat generation coefficient
 c_p specific heat at constant pressure
 C_w surface concentration
 T_w surface temperature
 Da is the Damköhler number
 t Time
 Q is the heat source
 g acceleration due to gravity

k' is the Darcy permeability
 b is the empirical constant
 $\pm v_0$ is the suction/blowing parameter
 Gr_c mass Grashof number
 Gr_τ thermal Grashof number
 Pr Prandtl number
 Sc Schmidt number
 Sh Sherwood number
 Nu Nusselt number
 Du Dufour number
 Sr Soret number
 $\beta\tau$ coefficient of thermal expansion
 βc coefficient of mass expansion
 ν Kinematic viscosity of the fluid
 ρ is the density of the fluid
 τ skin friction parameter
 α heat generation/absorption coefficient

δ Chemical reaction parameter

References

- [1] R.I. Tanner, Engineering Rheology, Oxford University Press, Oxford, 1992.
- [2] R. Nalim, K. Pekkana, H. B. Sun, and H. Yokota. Oscillating Couette flow for in vitro cell loading. *J. Biomech.*, 37, 939–942 (2004)
- [3] B.G. Prasad, and R. Kumar, Unsteady hydromagnetic Couette flow through a porous medium in a rotating system. *Theor. Appl. Mech. Lett.*, 1, 042005 (2011) DOI 10.1063/2.1104205
- [4] O.A. Beg, S.K Ghosh, and M. Narahari, Mathematical modeling of oscillatory MHD Couette flow in a rotating highly permeable medium permeated by an oblique magnetic field. *Chem. Engin. Commun.*, 198, 235–254 (2010)
- [5] O.A. Beg, H.S. Takhar, J. Zueco, A. Sajid, and Bhargava, R. Transient Couette flow in a rotating non-Darcian porous medium parallel plate configuration: network simulation method solutions. *Acta Mech.*, 200, 129–144 (2008)
- [6] G.S. Seth, M.S. Ansari, and R. Nandkeolyar, Effects of rotation and magnetic field on unsteady Couette flow in a porous channel. *J. Appl. Fluid Mech.*, 4, 95–103 (2011)
- [7] G.S. Seth, S.M. Hussain, and J.K. Singh, MHD Couette flow of class-II in a rotating system. *J. Appl. Math. and Bioinformatics*, 1, 31–54 (2011)
- [8] M. Guria, S. Das, R.N. Jana, and S.K. Ghosh, Oscillatory Couette flow in the presence of inclined magnetic field. *Meccanica*, 44, 555–564 (2009)
- [9] C. Fetecau, C. Fetecau, M. Kamran, and D. Vieru, Exact solutions for the flow of a generalized Oldroyd-B fluid induced by a constantly accelerating plate between two side walls perpendicular to the plate. *Int. J. Non-Newtonian Fluid Mech.*, 156, 189–201 (2009)
- [10] S. Abbasbandy, T. Hayat, H.R. Ghehsareh, and A. Alsaedi, MHD Falkner-Skan flow of a Maxwell fluid by rotational Chebyshev collocation method. *Appl. Math. Mech. Engl. Ed.*, 34(8), 921–930 (2013) DOI 10.1007/s10483-013-1717-7
- [10] T. Hayat, R.J. Moitsheki, and Abelman, S. Stokes' first problem for Sisko fluid over a porous wall. *Appl. Math. Comput*, 217, 622–628 (2010)
- [12] M. Khan, and J. Farooq, On heat transfer analysis of a magnetohydrodynamic Sisko fluid through a porous medium. *J. Porous Media*, 13, 287–294 (2010)
- [13] H.P. Rani, G.J. Reddy and C.N. Kim, Transient analysis of diffusive chemical reactive species for couple stress fluid flow over vertical cylinder. *Appl. Math. Mech. -Engl. Ed.*, 34(8), 985–1000 (2013) DOI 10.1007/s10483-013-1722-6
- [14] T. Hayat, S.A Shehzad and A. Alsaedi, Three-dimensional stretched flow of Jeffrey fluid with variable thermal conductivity and thermal radiation. *Appl. Math. Mech. - Engl. Ed.*, 34(7), 823– 832 (2013) DOI 10.1007/s10483-013-1710-7
- [15] T. Hayat, S. Abelman, C. Harley and A. Hendi, Stokes' first problem for a rotating Sisko fluid with porous space. *J. Porous Media*, 15, 1079–1091 (2012)
- [16] S. Gozde, M. Pakdemirli, T. Hayat, and Y. Aksoy, Boundary layer equations and Lie group analysis of a Sisko fluid. *J. Appl. Math.*, 2012, 259608 (2012)
- [17] T. Hayat, S. Nadeem, S. Asghar, A.M. Siddiqui, *Appl. Math. Eng.* 11 (2006) 415.
- [18] T. Hayat, A.H. Kara, *Math. Comput. Modell.* 43 (2006) 132.
- [19] T. Hayat, S.B. Khan, M. Khan, *Nonlinear Dyn.* 47 (2007) 353.
- [22] M.V. Karwe, Y. Jaluria, *ASME J. Heat Transfer* 113 (1991) 612–619.
- [23] A. Ahmed Afify, Similarity solution in MHD: Effects of thermal diffusion and diffusion thermo on free convective heat and mass transfer over a stretching surface considering suction or injection, *Commun Nonlinear Sci Numer Simulat* 14 (2009) 2202–2214
- [24] R. Tsai, J. S. Huang, Numerical study of Soret and Dufour effects on heat and mass transfer from natural convection flow over a vertical porous medium with variable wall heat fluxes, *Computational Materials Science* (2009)
- [25] A.W. Sisko, (1958). The flow of lubricating greases, *Industrial and Engineering Chemistry Research*, Vol. 50(12), pp. 1789-1792.
- [26] A.M. Siddiqui, A.R. Ansari, A. Ahmad, and N. Ahmad (late), (2009). On Taylor's scraping problem and flow of Sisko fluid, *Mathematical Modeling and Analysis* Vol. 14(4), pp. 515- 529.
- [27] K.S. Mekheimer, and M.A. El Kot, (2012). Mathematical modelling of unsteady flow of a Sisko fluid through an anisotropically tapered elastic arteries with time-variant overlapping stenosis, *Appl. Math. Modell*, doi:10.1016/j.apm.2011.12.051.
- [28] WC Tan and T. Masuoka, (2005a). Stokes first problem for second grade fluid in a porous half space. *Int. J. Non-Linear Mech.* 40, 515–522.
- [29] WC Tan, and T. Masuoka (2005b). Stokes first problem for an Oldroyd-B fluid in a porous half space. *Phys. Fluid* 17, 02101–023107.
- [30] U. Ascher, R. Mattheij, and R. Russell, "Numerical Solution of Boundary Value Problems for Ordinary Differential Equations." *SIAM Classics in Applied Mathematics*. Vol. 13. (1995).
- [31] U. Ascher, and L. Petzold, "Computer Methods for Ordinary Differential Equations and Differential-Algebraic Equations." *SIAM*, Philadelphia. 1998.

- [32] P.B. Bailey, L.F. Shampine and P.E. Waltman, Nonlinear Two Point Boundary Value Problems. New York: Academic Press, 1968.
- [33] W.E. Boyce and R.C. DiPrima, Elementary Differential Equations and Boundary Value Problems. New York: John Wiley & Sons, 1997.
- [34] J.R. Cash, "The Integration of Stiff IVP in ODE Using Modified Extended BDF." Computers and Mathematics with Applications. Vol. 9. (1983): 645-657.
- [35] C.W. Gear, Numerical Initial Value Problems in Ordinary Differential Equations. Prentice-Hall, 1971.

Biography

Dr. A. M. Okedoye is currently a senior lecturer in the department of Mathematics and Computer Science, Federal University of Petroleum Resources, Effurun (FUPRE), Delta State, Nigeria. He is a graduate of Pure and Applied Mathematics from Ladoke Akintola University of Technology, Ogbomoso, Nigeria in 1999. He also obtained M. Tech Applied Mathematics (Combustion Theory) and Ph.D Applied Mathematics (Fluid Dynamics) in 2004 and 2007 respectively, from the same university with special interest in numerical computation and computer programming. He is a member of International Association of Engineers (IAENG), Mathematical Association of Nigeria (MAN), Nigerian Association of Mathematical Physics (NAMP), Nigerian Mathematical Society (NMS) and African Mathematical Union (AMU). Dr. Okedoye has over forty publications in both local and international journals.